Characterization of FIM-FGFR1, the fusion product of the myeloproliferative disorder-associated t(8;13) translocation

Vincent Ollendorff, Géraldine Guasch, Daniel Isnardon, Rémi Galindo, Daniel Birnbaum, Marie-Josèphe Pébusque

THE JOURNAL OF BIOLOGICAL CHEMISTRY
Vol. 274, No. 38, Issue of September 17, pp. 26922–26930, 1999

Printed in U.S.A.

Characterization of FIM-FGFR1, the Fusion Product of the Myeloproliferative Disorder-associated t(8;13) Translocation*

(Received for publication, May 14, 1999, and in revised form, June 28, 1999)

Vincent Ollendorff‡§, Géraldine Guasch‡¶, Daniel Isnardon‖, Rémy Galindo, Daniel Birnbaum‡§‡‡, and Marie-Josèphe Pébusque‡ ‡‡**

*From the ‡Laboratoire d'Oncologie Moléculaire, U119 INSERM, Institut de Cancérologie et d'Immunologie, 27 Boulevard Leï Roure, 13009 Marseille, France, the §Laboratoire de Biologie des Tumeurs, Institut Paoli-Calmettes, Marseille 13009, France, ‖Unité d'Immunologie des Tumeurs, Institut Paoli-Calmettes, Marseille 13009, France, and the **Laboratoire de Biologie Cellulaire, Institut Paoli-Calmettes, Marseille 13009, France*

The t(8;13) translocation found in a rare type of stem cell myeloproliferative disorder generates a constitutively activated tyrosine kinase containing N-terminal sequence encoded by the *FIM* gene linked to the FGFR1 kinase domain. Here we have further characterized FIM and FIM-FGFR1 proteins. Firstly, we have studied their respective subcellular localization. We show that FIM has nuclear and nucleolar localization, whereas FIM-FGFR1 is mainly cytoplasmic. Within the nucleolus, FIM colocalizes with the upstream binding factor in interphasic cells, indicating that FIM may be involved in the regulation of rRNA transcription. We demonstrate that the targetting of FIM to the nucleus depends upon its C-terminal region, which is absent in the cytoplasmic FIM-FGFR1 protein. Secondly, we demonstrate that FIM-FGFR1 has constitutive dimerization capability mediated by the FIM N-terminal sequences. Finally, we show that FIM-FGFR1 promotes survival of pro-B Ba/F3 cells after interleukin-3 withdrawal, whereas ligand-activated FGFR1 induced not only cell survival but also interleukin-3 independence. Taken together, these results indicate that FIM-FGFR1 is activated by dimerization as a cytoplasmic kinase and suggest that FIM-FGFR1 partially signals through the FGFR1 pathways.

A stem cell myeloproliferative disorder with a multilineage involvement that suggests transformation of a primitive hematopoietic stem cell is associated with three different translocations with a breakpoint in region p11–12 of chromosome 8: t(6;8)(q27;p11), t(8;9)(p11;q33), and t(8;13)(p12;q12), respectively (1). On chromosome arm 8p, it involves in each case the rearrangement of the *FGFR1* gene (2), which encodes a transmembrane tyrosine kinase receptor for members of the fibroblast growth factor family (3). We have cloned the partner genes of *FGFR1* on chromosomes 6q27, 9q33, and 13 q12. They are novel and unrelated genes named *FOP* (4), *CEP110*,[1] and *FIM* (fused in myeloproliferative disorders) (5). The 13q12 breakpoint gene has also been partially characterized by others and named *ZNF198* (6, 7) and *RAMP* (8).

FIM ubiquitous transcript encodes a protein of 1379 amino acid residues (5) that shows several motifs: a N-terminal cysteine-rich region containing 10 repeats with the consensus sequence C-X_2-C-X_{18-24}-(F/Y)-C-X_3-C that corresponds to a novel type of zing finger motifs, a highly hydrophobic, proline-rich stretch, and two putative nuclear localization signals (NLSs)[2] in the C-terminal region. *FIM* displays similarity with *DXS6673E*, a candidate gene for X-linked mental retardation at Xq13.1 (9).

The *FIM-FGFR1* transcript encodes an aberrant tyrosine kinase of approximately 150 kDa (5, 10). The FIM-FGFR1 fusion protein contains the N-terminal two-thirds of FIM, retaining the 10 putative zinc finger motifs and the FGFR1 intracellular region minus the major part of the juxtamembrane domain. We previously showed that it has a constitutive tyrosine kinase activity (5). Constitutive activation of a tyrosine kinase receptor by permanent, ligand-independent stimulation can lead to aberrant stimulation of signal transducing pathways, resulting in cellular transformation and neoplasia (11). The FGFR1 tyrosine kinase receptor is broadly expressed and may play a role in many different processes, including hematopoiesis (12). Because of constitutive activation, the fusion protein is likely to cause aberrant signaling rather than simple ectopic activation of a normal FGFR1 pathway.

Because tyrosine kinase receptors are known to be activated following dimerization or higher order oligomerization (13) and because each of the FGFR1 fusion partners, *i.e.* FIM, FOP, or CEP110, shows potential dimerization motifs in its N-terminal region, we suspected that FIM-FGFR1 constitutive kinase activity (5) is triggered by ligand-independent dimerization involving the FIM N-terminal region, especially its zinc finger motifs. Indeed, the latter are binding motifs that very frequently mediate protein-protein (in addition to DNA-protein) interactions and can create homodimerization (14).

Here we gather clues about the mechanism of action of the FIM-FGFR1 fusion protein that may sustain its oncogenic potential in hematopoietic cells. In particular, we demonstrate that FIM-FGFR1 fusion protein is localized in the cytoplasm and that its dimerization is mediated by the N-terminal FIM sequences. We also present data supporting the idea that FIM-FGFR1 could act on cell survival.

* This work was supported by INSERM, Institut Paoli-Calmettes, and grants from Ligue Nationale Contre le Cancer (National and Var committees) and from Groupement des Entreprises Françaises dans la Lutte contre le Cancer. The costs of publication of this article were defrayed in part by the payment of page charges. This article must therefore be hereby marked "*advertisement*" in accordance with 18 U.S.C. Section 1734 solely to indicate this fact.

¶ Recipient of a fellowship from MESR.

‡‡ To whom correspondence may be addressed: Laboratoire d'Oncologie Moléculaire, U.119 INSERM, Institut de Cancérologie et d'Immunologie 27 Bd Leï Roure, 13009 Marseille, France. Tel.: 33-4-91-75-84-07; Fax: 33-4-91-26-03-64; E-mail: pebusque@marseille.inserm.fr or birnbaum@marseille.inserm.fr.

[1] Guasch, G., Mack, G., Popovici, C., Dastugue, N., Birnbaum, D., Rattne, B. J., and Pébusque, M.-J., submitted for publication.

[2] The abbreviations used are: NLS, nuclear localization signal; IL, interleukin; kb, kilobase pair(s); HA, hemagglutinin; PBS, phosphate-buffered saline; UBF, upstream binding factor.

EXPERIMENTAL PROCEDURES

Cells and Culture Conditions—Cos-1 cells were maintained in Dulbecco's modified Eagle's medium with 10% new born calf serum in a 5% CO_2 incubator at 37 °C. Murine Ba/F3 cells from a lymphoid pro-B-cell line dependent on IL-3 for survival and proliferation (15, 16) were maintained in RPMI 1640 medium with 10% fetal bovine serum supplemented with IL-3 in a 5% CO_2 incubator at 37 °C.

DNA Constructs—All constructs were derived from the wild type *FIM* (pFIM) and fusion *FIM-FGFR1* (pCHIM) cDNAs inserted in the pcDNA3 expression vector (Invitrogen) as described in a previous work (5) and corresponding to an exon splicing from nucleotides 492 to 753 of the *FIM* long form (EMBL accession number Y13472). The respective positions of nucleotides and amino acids for all the constructs mentioned below (either wild type or chimeric) correspond to the FIM sequence from ATG minus the 261-base pair alternatively spliced. A sequence encoding the Myc epitope tag, MEQKLISEEDL, (17, 18), preceded by a Kozak sequence was added at the 5′ of pFIM and pCHIM constructs and renamed mycFIM and mycCHIM, respectively. All constructs were made using standard techniques. Each construct was sequenced to verify the correct frame as well as the proper sequence of any linker introduced during the cloning procedure.

The two-hybrid plasmids (pBTM116 and pVP16) were a generous gift from S. Hollenberg and J. A. Cooper (Fred Hutchinson Cancer Research Center, Seattle, WA). To facilitate the cloning procedure, the polylinker region of both pBTM116 and pVP16 vectors has been remodeled to make three different versions of pBTM116 and pVP16 (*i.e.* A, B, and C), differing in-frame at the *Bam*HI site and containing an additional *Not*I site as described in Ollendorff and Donoghue (19). *FIM* or *CHIM* (corresponding to *FIM-FGFR1*) cDNAs were cloned in-frame with either LexA (in pBTM116) or VP16 (in pVP16). Six different FIM constructs were generated: L-FIM (24–1292), corresponding to a 3.8-kb *Nco*I/*Not*I fragment derived from mycFIM and inserted in pBTM-C cut by *Bam*HI and filled in with the Klenow polymerase; V-FIM (24–1292), corresponding to a *Not*I/*Sal*I fragment derived from L-FIM (24–1292) and ligated in the *Not*I/*Sal*I sites of pVP16-C; L-FIM (314–1292), corresponding to a 3-kb *Eco*RI fragment derived from pFIM (FIM full-length cloned in pBluescript SK) and ligated in the *Eco*RI site of pBTM-A; V-FIM (314–1292), corresponding to a 3-kb *Bam*HI/*Sal*I fragment from L-FIM (314–1292) inserted in the *Bam*HI/*Sal*I sites of pVP16-A; L-FIM (24–425), corresponding to a 1.2-kb *Hin*dIII filled in/*Not*I fragment, which contains the sequences encoding the N-terminal sequence of *FIM*, derived from L-FIM (24–1292), and ligated into the *Eco*RI filled in/*Not*I sites of pBTM-C; and V-FIM (24–425), corresponding to a 1.2-kb *Not*I/*Sal*I fragment derived from L-FIM (24–425), and introduced in pVP16-C. Seven *FIM-FGFR1* plasmids were constructed as follows: L-CHIM (24–1218), a 4.2-kb *Nco*I/*Not*I fragment containing the full-length coding sequence of *FIM-FGFR1* was derived from mycCHIM filled in with Klenow and ligated in *Bam*HI filled in site of pBTM-C; V-CHIM (24–1218), the 4.2-kb *Not*I/*Sal*I fragment from L-CHM (24–1218) was prepared and ligated into pVP16-C; L-CHIMKD (24–1218) (kinase dead), because the *FIM-FGFR1* fused to LexA (construct L-CHIM (24–1218) constitutively transactivated the reporter genes of the L40 yeast strain, a kinase-defective mutant *FIM-FGFR1* fused to LexA was made by site-directed mutagenesis using Quickchange kit (Stratagene) according to the manufacturer's recommendations changing lysine 910 (lysine 514 in the FGFR1 sequence) to alanine (20) in the L-CHIM (24–1218); L-CHIM (314–1218), a 3-kb *Eco*RI fragment was derived from L-CHIM (24–1218) and inserted in the *Eco*RI site of pBTM-A; V-CHIM (314–1218), a 3-kb *Not*I/*Sal*I fragment derived from L-CHIM (314–1218) was inserted in pVP16-A; L-CHIM (425–1218), a 2.7-kb blunt end *Hin*dIII/*Not*I fragment was derived from mycCHIM and inserted into pBTM-A; and V-CHIM (425–1218), the 2.7-kb *Not*I/*Eco*RI fragment was inserted in *Bam*HI filled in site of pVP16-A. These LexA and VP16 CHIM (425–1218) fusion constructs are deleted of the N-terminal FIM region and retain only 6 of the 10 zinc fingers motifs present in FIM. For CHIMKD (425–1218), as with the previously described construct L-CHIM (24–1218), L-CHIM (425–1218) activated constitutively the reporter genes in yeast. To prevent this we made a L-CHIMKD (425–1218) by swapping a 1.65-kb *Nhe*I/*Eco*RI fragment from L-CHIM (425–1218) by the corresponding region in L-CHIMKD (24–1218) encompassing the $Lys^{910} \rightarrow$ Ala mutation. As a result, the construct L-CHIMKD (425–1218) did not show any constitutive reporter transactivation.

FIM N-terminal constructs consisting of the deletion of sequences encoding either one or two putative C-terminal FIM NLSs, DC1 and DC2, respectively, were made as follows. DC1 was deleted of *FIM* sequences coding for the C-terminal putative bipartite NLS (amino acids 1, 163–1, and 197). Briefly, mycFIM was cut with *Xho*I (unique site in *FIM*, nucleotide position 3329) and *Apa*I (polylinker). Synthethic oligonucleotides with cohesive *Xho*I/*Apa*I and an in-frame stop codon were inserted by ligation. DC2 was deleted of the *FIM* sequences encoding the two putative NLSs [the previously described bipartite NLS and the one located between amino acid #954 and #964 (PRSKKKGAKRK)]. Briefly, mycFIM was cut with unique *Eco*RV *FIM* site (nt position 2, 760) and *Not*I (polylinker) and oligonucleotides with cohesive *Eco*RV/*Not*I sites and containing an in-frame stop codon were ligated in.

FIM C-terminal plasmids that contain the sequences coding for either one or two of the putative C-terminal NLSs of *FIM*, DN1 and DN2, respectively, were constructed in the RK5-myc vector (a kind gift from J. P. Borg *et al.* (21)) as follows. For DN1, a 850-base pair *FIM* restriction fragment containing the sequences coding for C-terminal FIM region with the putative bipartite NLS from unique *Pvu*II *FIM* site (nucleotide position 3091) and *Xba*I (mycFIM polylinker) was filled in (with Klenow) and inserted in the RK5-myc cut by *Xba*I filled in. For DN2, similarly, a Myc-tagged construct retaining C-terminal sequences including both NLSs was made by inserting a 1200-base pair *FIM* restriction fragment from *Eco*RV (nucleotide position 3021) and *Xba*I (polylinker) in the plasmid RK5-myc cut by *Eco*RI and filled in with Klenow.

HA-tagged FIM-FGFR1 expression vectors were cloned in pcDNA3 in-frame with three repeats of the HA epitope (pcDNA3HA) (Invitrogen) as follows. For HACHIM, a near full-length coding sequence of 4.1-kb fragment (fragment *Nco*I filled in *Not*I (polylinker) derived from the mycCHIM was cloned into pcDNA3HA vector cut by *Xba*I and blunt ended. For HAΔR1CHIM, a 3-kb *Eco*RI (nucleotide position 1200)/*Xho*I (polylinker) fragment from mycFIM-FGFR1 and retaining the sequences coding for 8 of the 10 zinc fingers was subcloned in pcDNA3HA vector. For HAΔHd3CHIM, similarly, a 2.7-kb *Hin*dIII/*Not*I (polylinker) filled in fragment from mycFIM-FGFR1 containing *FIM* sequences coding for 6 of the 10 zinc finger motifs was inserted in the pcDNA3HA vector cut with *Eco*RV. For pFGFR1A, the full-length *FGFR1* cDNA was excised from pFlg16 (22) by digestion with *Apa*I and *Nco*I and was inserted in the *Apa*I-*Eco*RV sites of pcDNA3 by blunt end ligation.

Transfection—Cos-1 cells were transiently transfected using 2 μg of plasmid DNA and 3 μl of FuGENE 6 transfection reagent (Roche Diagnostics, Meylan, France) following the manufacturer's recommendations. Ba/F3 cells were electroporated as follows. 1×10^7 cells were washed in phosphate-buffered saline (PBS) and incubated for 10 min at room temperature with 20 μg of plasmid DNA at 350 mV/960 microfarad in a Bio-Rad apparatus. Following a 10-min incubation at room temperature, cells were seeded in plates.

Selection of Stable Transfected Clones—After electroporation, Ba/F3 cells were plated in 10 ml of IL-3 medium for 24 h and then selected in IL-3 medium plus 1 mg of G418/ml. Neomycin-resistant cells were subcloned by limiting dilution. FGFR1 positive cells were selected in G418 medium containing 10 ng/ml of FGF1 plus 10 μg/ml of heparin (22) and refed every 2 days. Stably transfected clones were selected 15 days after culture.

Antibodies—The DSKITPSSKELASQK peptide, corresponding to amino acids 96–111 of FIM sequence, was chosen for chemical synthesis (Neosystem, Strasbourg, France) owing to its predicted antigenicity. This peptide was coupled to keyhole limpet hemocyanin as hapten, suspended in PBS, and used to immunize rabbits by intramuscular and subcutaneous injections. The antibody generated against this peptide was designated anti-N-FIM.

The mouse monoclonal anti-Myc (9E10) (17) and anti-phosphotyrosine 4G10 antibodies were purchased from Santa Cruz Biotechnology, Inc. and Upstate Biotechnology, Inc. (Lake Placid, NY), respectively. The anti-Myc was revealed by an Alexa-conjugated anti-mouse antibody (Molecular Probes, Oregon, WA).

Human autoimmune serum characterized on purified UBF (23) was kindly provided by D. Hernandez-Verdun (Paris, France). UBF labeling was revealed by a fluorescein isothiocyanate-conjugated anti-human antibody (Immunotech, Marseille, France).

Immunofluorescence Analysis—Cos-1 cells were grown as monolayer on coverslips 1 day before transfection (1 to 2×10^5 cells/60-mm plate). 24 h after transfection, cells were washed once in PBS and fixed in 3.7% paraformaldehyde in 1× PBS for 15 min at room temperature. After extensive PBS washes, cells were permeabilized and blocked in 5% fetal calf serum/PBS, 0.1% Triton X-100 for 15 min. Cells were incubated with anti-Myc antibody used at a final concentration of 1 μg/ml for 1 h at room temperature, rinsed several times in 1× PBS, and then incubated with 2 μg/ml of the Alexa-conjugated anti-Mouse secondary antibody.

To detect the endogenous FIM protein, transfected Cos-1 cells were incubated with the antipeptide serum anti-N-FIM (dilution, 1:1000 or 1:5000) for at least 1 h. This antibody was revealed either by an Alexa-conjugated anti-rabbit (Molecular Probes) or Texas Red-conjugated goat anti-rabbit antibodies (Molecular Probes). Controls were made by preincubating the FIM antiserum with the immunogen peptide (50 μM) or by incubating the cells with a preimmune serum rather than the anti-N-FIM serum. In these cases, the immunofluorescence staining was abolished, confirming the specificity of anti-N-FIM antiserum signal.

To detect UBF, cells were incubated with anti-UBF serum used at the final dilution of 1:100 or 1:200 as described in Roussel *et al.* (24). The antibody was then revealed by a goat fluorescein isothiocyanate anti-human antibody (Immunotech).

For FIM and UBF double labeling immunofluorescence, cells were first incubated with the two respective primary antibodies and then washed in PBS. The coverslips were then incubated with a Goat anti-human fluorescein isothiocyanate to detect UBF, washed several times, and incubated with a goat Texas Red anti-rabbit antibody to detect FIM. The staining pattern observed for endogenous FIM after single labeling was identical to the double stained cells experiment, ruling out any cross-reactions between secondary antibodies.

Except for the double labeling of UBF and FIM, after the secondary antibody incubation, coverslips were washed several times in PBS and incubated for 10 min in PBS containing 1 μg/ml of ethidium-acridine heterodimer (Molecular Probes) used to visualize DNA (25, 26). After several washes with PBS, coverslips were then mounted in Mowiol. Cellular localization of proteins was analyzed by confocal laser system microscopy using a TCS NT Leica apparatus (Heidelberg, Germany).

Yeast Two-hybrid Interactions—The two-hybrid interaction assays were done according to previously published protocols using the *Saccharomyces cerevisiae* L40 strain (27, 28). Plasmid encoding a fusion between the DNA binding domain LexA and the construct of interest was cotransformed in the L40 strain with a plasmid encoding a fusion between the activation domain VP16 and a second protein of interest. After growth of the double transformants on selective media (−Trp, −Leu plates), several individual transformants were tested for their ability to activate the two integrated reporter genes *HIS3* and *LACZ*. An interaction was scored positive based on whether or not yeast colonies were able to grow after 3–5 days at 30 °C on −His, −Trp, −Leu plates containing 10 mM of 3-amino-triazol (Sigma). The β-galactosidase activity was also checked qualitatively by a filter assay as described (28).

We first noticed that a LexA fusion with the chimeric FIM-FGFR1 protein was able to activate the reporter genes constitutively rending impossible the two hybrid analysis (data not shown). However, we observed that making a LexA fusion of CHIM with a point mutant that eliminates any tyrosine kinase activity of the FGFR1 kinase abolished this constitutive gene reporter transactivation. Therefore, we used as chimeric LexA fusions only kinase inactive (kinase dead or KD) derivatives for the two-hybrid analysis (L-CHIMKD (24–1218) and L-CHIMKD (425–1248)).

Cell Lysis, Immunoprecipitation, and Western Blotting—Cell lysates from 2×10^6 Ba/F3 cells expressing the wild type or fusion proteins and immunoprecipitation using the antibody anti-C-FGFR1 were done as described (29).

For dimerization studies, 1×10^6 Cos-1 cells were split in 100-mm plates, and transfected 24 h later using FuGENE-6 (as a ratio of 2 μl of FuGENE-6/1 μg of plasmid DNA). One day after transfection, cells were washed on ice with cold PBS and lysed in 1 ml of lysis buffer as described (21) containing protease inhibitors (1 mM phenylmethylsulfonyl fluoride, 5 μg/ml aprotinin, 10 μg/ml leupeptin, 6 μg/ml antipain, and 10 μg/ml pepstatin) and spun for 10 mn at 4 °C to remove debris. Immunoprecipitation was done overnight at 4 °C on 600 μl of total cell lysate with the anti-Myc monoclonal antibody (9E10). Immunoprecipitates were collected on protein A-Sepharose beads for 1 h, washed three times in the same lysis buffer, and resuspended in 60 μl of sample buffer.

Samples were boiled for 5 min, and half of each immunoprecipitate was loaded on 7.5% SDS-polyacrylamide gel electrophoresis, transferred to membrane (Hybond-C; Amersham Pharmacia Biotech), and immunoblotted following blocking in bovine serum albumin 5% with either anti-phosphotyrosine or anti-Myc or anti-HA (3F10, Roche) or anti-C-FGFR1 (C15, Santa Cruz Biotechnology) antibodies. Blots were visualized using chemiluminiscence (Amersham Pharmacia Biotech).

Cell Survival and Proliferation Assays—For growth curves, 1×10^4 nontransfected Ba/F3 cells or neomycin-resistant cells expressing either *FIM-FGFR1* or *FGFR1* or transfected with empty vector were plated on day 0, and viable cells were counted by trypan blue exclusion 6, 24, 48, and 72 h after culture with or without IL-3. Ba/F3 cells expressing FGFR1 were cultured in the presence of 10 ng/ml of FGF1 plus 10 μg/ml of heparin. Cell proliferation was monitored by [^{3}H]thymidine uptake. Cultures of 1×10^4 cells from the same clones (*FIM-FGFR1*, *FGFR1*, or without any insert) were grown in 96-well plates with the same conditions as described above. After 6, 24, 48, and 72 h, 0.74 MBq of [^{3}H]thymidine was added to each well for 6 h. Incorporated radioactivity was estimated by liquid scintillation counting.

DNA Labeling and Flow Cytometry Analysis—In parallel with trypan blue staining, cell loss was determined by a flow cytometry assay as described in Nicoletti *et al.* (30). Briefly, after cell culture of the selected clones as described above, 100% ethanol fixation, RNase treatment, and propidium iodide staining, the DNA content of cell nuclei was determined using a FACScan cytometer (Becton Dickinson FACScan). Subdiploid cells were considered apoptotic cells.

RESULTS

FIM-FGFR1 Is a Cytoplasmic Protein, Whereas FIM Is Nuclear—The fusion between two proteins resulting from a chromosomal translocation event often creates an aberrantly located protein. This abnormal subcellular localization can be, at least in part, the source of its oncogenic effect. Based on sequence analyses, we predicted the cytoplasmic localization of FIM-FGFR1 fusion protein because it lacks the FGFR1 transmembrane domain and the two putative NLSs present in the C terminus of the wild type FIM (5). To test this prediction, we compared the localization of both fusion FIM-FGFR1 and wild type FIM proteins by immunofluorescence in Cos-1 cells transiently transfected with the corresponding Myc-tagged constructs. As suspected, the FIM-FGFR1 fusion protein was mostly located in the cytoplasm (Fig. 1*A*, *panels a* and *c*). In contrast, the FIM protein was found exclusively located within the cell nucleus, in the nucleoplasm, and in discrete nucleolar areas (Fig. 1*B*, *panels a*, *c*, *d*, and *f*). One nuclear pattern recurrently observed is shown in detail (Fig. 1*B*, *panels d–f*). Therefore the FIM-FGFR1 fusion protein resulting from the t(8;13) translocation is mainly translocated to a subcellular compartment different from both FIM and FGFR1 wild type proteins, which are nuclear and plasma membrane bound, respectively.

FIM C-terminal Region Contains Two Functional NLSs—FIM C-terminal sequence displays two putative nuclear localization signals (Fig. 1, *dark* and *light blue boxes*), the more C-terminal one being bipartite (5). To demonstrate that these nuclear localization sequences are actually important, we studied the localization of different FIM proteins (Fig. 2). Two short C-terminal deletion constructs, named DC1 and DC2, were first studied. The respective truncated proteins lack one and two putative nuclear localization signals, respectively (Fig. 2, *A* and *B*). Eliminating the FIM C-terminal region containing the putative bipartite NLS greatly affected the localization of the protein, which showed a cytoplasmic pattern in most cells (Fig. 2*A*, *panels a–c*). However, in some cells the localization of this truncated protein was partially nuclear, suggesting that another signal localization could still be functional (Fig. 2*A*, *panels d–f*). Indeed, the localization of the DC2 protein, which lacks the two putative NLSs, was exclusively cytoplasmic (Fig. 2*B*), either remaining diffuse (Fig. 2*B*, *panels d–f*) or concentrated in aggregates (Fig. 2*B*, *panels a–c*). These results suggest that the two FIM NLSs are functional.

We then studied the localization of reciprocal proteins, DN1 and DN2, containing FIM C-terminal sequences with either one or two of the NLSs, respectively. DN1 protein displayed a mixed nuclear and cytoplasmic localization (Fig. 2*C*), indicating that this region alone containing the bipartite NLS was able to target the protein to the nuclear compartment although quite imperfectly. In contrast, the localization of the protein bearing the FIM C terminus including the two NLSs (DN2) was

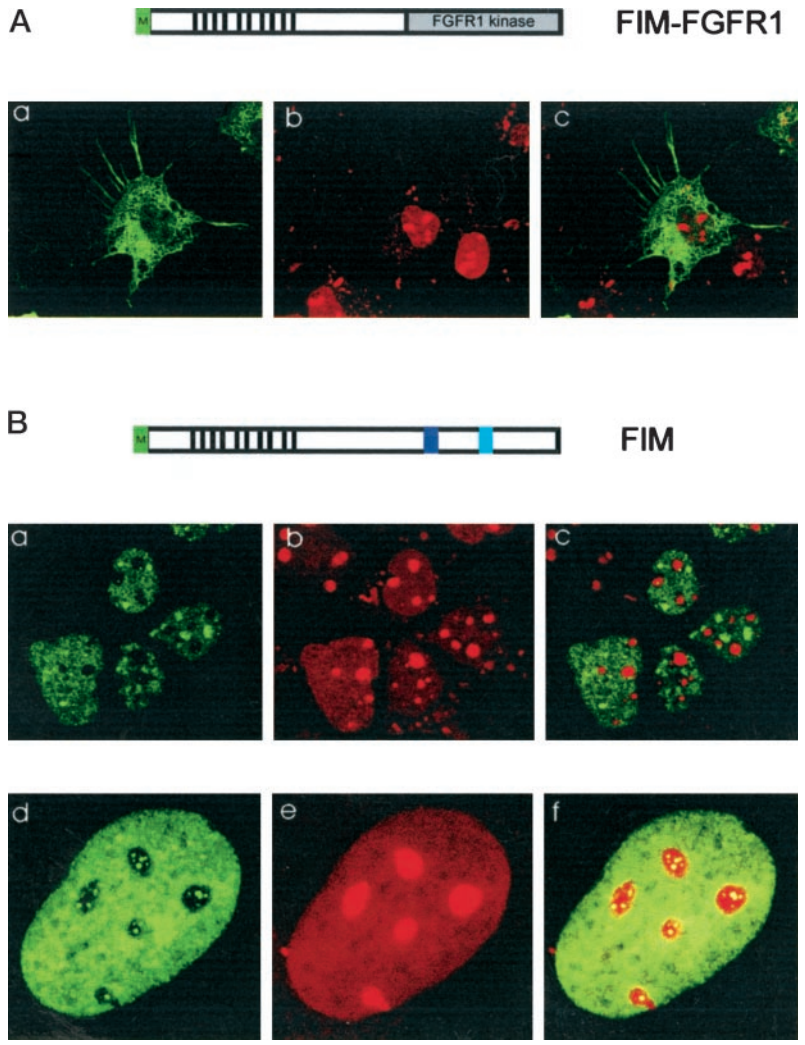

FIG. 1. **Immunolocalization of mycFIM-FGFR1 and mycFIM.** mycFIM-FGFR1 (*A*) and mycFIM (*B*) expression constructs are shown above each panel; both contain a Myc epitope tag at their N terminus (*green box*). The *black bars* represent the 10 putative zinc fingers of the N-terminal FIM region. The FGFR1 kinase is shown in *gray*, and the two putative nuclear localization signals present in the C-terminal region of FIM are represented as *dark* and *light blue boxes*, respectively. Transfected Cos-1 cells were grown on coverslips and subjected to double staining immunofluorescence with anti-Myc antibody, revealed by Alexa-conjugated anti-mouse secondary antibody and ethidium acridine to visualize mycFIM-FGFR1 and mycFIM (in *green*) and the DNA (in *red*), respectively. Magnifications: *A*, 630×; *B*, *panels a–c*, 1000×; *panels d–f*, 3000×.

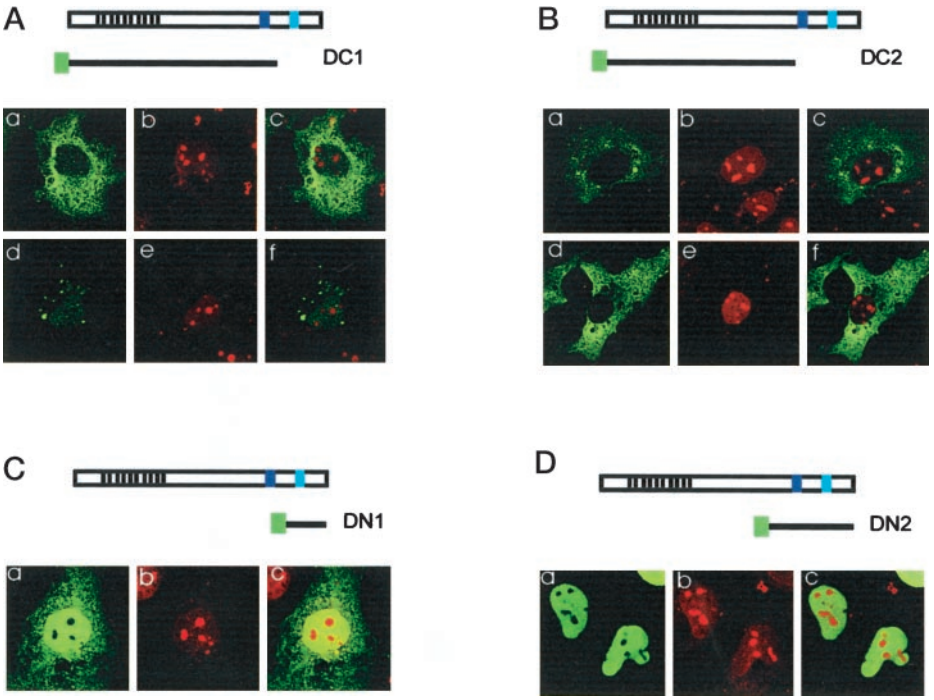

FIG. 2. **Mapping of the nuclear localization signal of FIM by immunofluorescence.** The immunolocalization of four Myc-tagged FIM deletions constructs were determined by immunofluorescence staining, as described in legend to Fig. 1. DC1 (*A*) and DC2 (*B*) are truncated FIM proteins deleted in their C termini of one or two putative NLSs, respectively. DN1 (*C*) and DN2 (*D*) are truncated FIM proteins deleted of a large portion of the molecule but retaining one and two putative NLS, respectively. Magnifications: 1000×.

exclusively nuclear in most cells (Fig. 2*D*). This result suggests that the other NLS, not examined here in isolation, is capable of directing nuclear localization of FIM. Altogether, these results indicate that two functional NLSs are present in the C-terminal region of FIM and that they are likely to cooperate to target FIM to the nucleus.

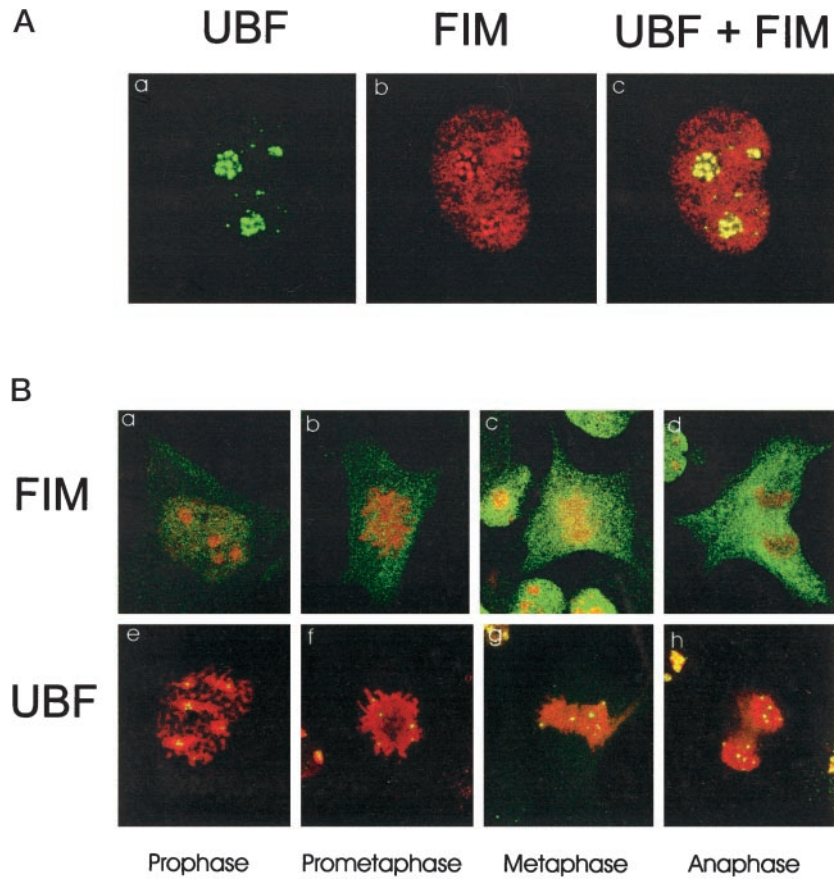

FIG. 3. **Immunolocalization of endogenous FIM during interphase or M phase in Cos-1 cells.** *A*, localization during interphase of endogenous UBF in the nucleolus (*panel a*) and endogenous FIM (*panel b*) in the nucleus and nucleolus and colocalization of the two proteins (*panel c*) using double staining with anti-N-FIM and anti-UBF human antibodies. Texas Red-conjugated anti-rabbit and fluorescein conjugated anti-human antibodies were used as secondary antibodies to detect endogenous FIM (in *red*) and UBF (in *green*), respectively. The *yellow color* in the overlapping image (*panel c*) represents the colocalization of FIM and UBF proteins in the nucleoli. *B*, localization during mitosis phase of FIM (*panels a–d*) and UBF (*panels e–h*). Endogenous FIM, detected with anti N-FIM antiserum followed by incubation in Alexa-conjugated anti-rabbit antibody (in *green*), is dispersed within the cytoplasm from prophase to anaphase (*panels a–d*). Endogenous UBF was detected as described for *A* and is seen as concentrated *yellow* and *green dots* attached to chromosome (*panels e–h*). Ethidium acridine was used to visualize the condensed M phase chromosomal DNA in *red*. Magnifications: *A*, 3000×; *B*, 1000×.

Endogenous FIM Exhibits a Nuclear and a Nucleolar Localization—To confirm the localization of FIM within the cell nucleus, we studied the distribution of the endogenous FIM by immunofluorescence with a polyclonal anti-N-FIM antibody (Fig. 1*B*). Endogenous FIM was found in the same localization as transfected mycFIM (Fig. 3*A*, *panel b*), *i.e.* not only throughout the nucleoplasm but also as concentrated dots in the nucleoli.

To precisely define the location of endogenous FIM in nucleoli, we studied its potential colocalization with the UBF, one of the elements of the multimeric protein complex required for rDNA transcription (for review see Ref. 31). During interphase, UBF was detected in discrete foci arranged in a necklace-like pattern (Fig. 3*A*, *panel a*), as described previously by others (23, 32). Colocalization of UBF and FIM proteins was visualized as overlapping nucleoli dots in yellow (Fig. 3*A, panel c*). However, during mitosis the localization of the two proteins was different. From early prophase to anaphase, endogenous FIM was diffuse in the cytoplasm, excluded from the condensed DNA (Fig. 3*B*, *panels a–d*, respectively). In contrast and as expected, UBF remained associated with the condensed chromosomes at all phases of the mitosis (Fig. 3*B, panels e–h*). Therefore, endogenous FIM and UBF colocalized only during interphase.

FIM N-terminal Motifs Are Able to Trigger Dimerization—To establish whether or not the FIM N-terminal region is responsible for dimerization and subsequent activation of the FGFR1 kinase, two types of approaches were used, *i.e. in vitro* using the two-hybrid system in yeast and *in vivo* by Cos-1 cotransfection experiments with FIM-FGFR1 constructs bearing two different N-terminal epitope tags.

We first used the two-hybrid system. For this purpose, we made several constructs with either FIM or FIM-FGFR1, fused to either the LexA DNA binding domain or the VP16 activation domain. Following cotransformation in the L40 yeast strain containing two integrated reporter genes (*HIS3* and *LACZ*), the interactions between a LexA fusion construct and a VP16 fusion construct were determined by testing several independent clones on plates depleted of histidine (see "Experimental Procedures"). Full-length FIM protein as a LexA fusion protein interacted with itself as a VP16 fusion (L-FIM (24–1292)/V-FIM (24–1292)) showing that FIM is able to dimerize (Fig. 4*A*). A series of two-hybrid constructs was made to delineate the region necessary for dimerization. A strong two-hybrid interaction was observed whenever the N terminus was present (L-FIM (24–425)/V-FIM (24–425); L-FIM (24–425)/V-FIM (24–1292); L-FIM (24–1292)/V-FIM (24–425)), demonstrating that this region, which contains 4 of the 10 zinc finger motifs, is sufficient to observe an interaction between two FIM proteins. In contrast, deleting this N-terminal region (L-FIM (314–1292)) either abrogated (L-FIM (314–1292)/V- (314–1292)) or severely reduced the interaction between two FIM proteins (L-FIM (314–1292)/V-FIM (24–1292)), confirming that the interaction between two FIM proteins takes place within the N-terminal FIM region (amino acids 24–425). In summary, these results indicate that two FIM proteins can interact through their respective N-terminal region.

FIM-FGFR1 Is Able to Dimerize—Because FIM-FGFR1 contains the N-terminal region of FIM that triggers the dimerization, several FIM-FGFR1 constructs (called CHIM) were similarly analyzed by the two-hybrid system (Fig. 4*B*). As predicted, two CHIM proteins containing the N-terminal region of FIM were able to dimerize (L-CHIMKD (24–1218)/V-CHIM (24–1218)). Like for the FIM proteins, this dimerization was essentially dependent on the presence of N-terminal sequences because a deletion of this region inhibited the two-hybrid interaction with N-terminal deletions (V-CHIM (314–1218) and V-CHIM (425–1218)). However, a weak interaction is still

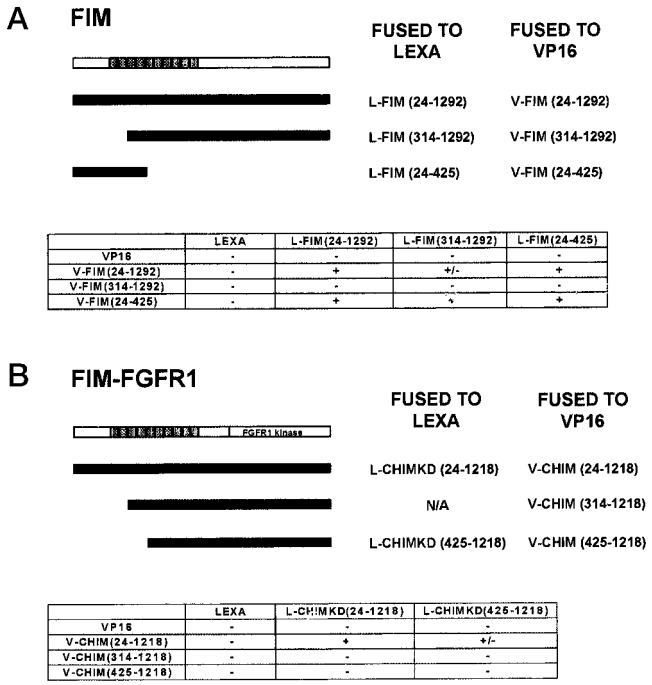

	LEXA	L-FIM(24-1292)	L-FIM(314-1292)	L-FIM(24-425)
VP16	-	-	-	-
V-FIM(24-1292)	-	+	+/-	+
V-FIM(314-1292)	-	-	-	-
V-FIM(24-425)	-	+	-	+

	LEXA	L-CHIMKD(24-1218)	L-CHIMKD(425-1218)
VP16	-	-	-
V-CHIM(24-1218)	-	+	+/-
V-CHIM(314-1218)	-	-	-
V-CHIM(425-1218)	-	-	-

FIG. 4. **Yeast two-hybrid assays detect FIM/FIM and FIM-FGFR1/FIM-FGFR1 interactions.** Human *FIM* and *FIM-FGFR1* cDNAs were used to derive all constructs seen in *A* and *B*, respectively. *Gray boxes* represent the positions of the FIM zinc finger motifs. The different constructs, fused to either LexA or VP16 (see "Experimental Procedures"), are indicated as L- or V-, respectively, followed by the amino acid limits of either FIM or FIM-FGFR1 (CHIM) proteins (in *parentheses*). The *S. cerevisiae* strain L40 was cotransformed with a combination of LexA and VP16 fusions, and individual colonies were tested for growth on minus histidine plates containing 10 mM 3-amino-triazol. β-Galactosidase activity was also qualitatively checked. The results of the two-hybrid FIM/FIM interactions (*A*) and FIM-FGFR1/FIM-FGFR1 (CHIM/CHIM) interactions (*B*) are summarized in the *tables*. N/A, not applicable.

detectable between L-CHIMKD (425–1248) and the full-length FIM-FGFR1 (V-CHIM (24–1218)) (Fig. 4*B*), indicating that in the absence of the N-terminal region the remaining zinc fingers are still capable of triggering dimerization. In conclusion, the two-hybrid results demonstrate that, as demonstrated for the FIM wild type proteins, the FIM-FGFR1 proteins are able to dimerize and that the N-terminal region is mainly responsible for this dimerization.

FIM-FGFR1 Fusion Proteins Dimerize in Vivo—To further establish that FIM-FGFR1 is able to dimerize, we cotransfected Cos-1 cells with constructs tagged with either Myc or HA epitope tags (Fig. 5*A*). Following immunoprecipitation with an anti-Myc antibody and Western blotting using an anti-HA antibody, we observed that HAFIM-FGFR1 was coimmunoprecipitated with mycFIM-FGFR1 (Fig. 5*B*, *lane 4*). N-terminal deletions of HAFIM-FGFR1 protein diminished its ability to dimerize with a full-length mycFIM-FGFR1 protein (Fig. 5*B*, *lanes 5* and *6*). As seen in the two-hybrid analysis, a FIM-FGFR1 protein deleted in its N-terminal portion is still able to interact weakly with a full-length FIM-FGFR1. In conclusion, the two-hybrid analysis and coimmunoprecipitation experiment demonstrate that the chimeric FIM-FGFR1 kinase is able to dimerize *in vivo* through its N-terminal FIM region and that the region (amino acids 25–425) is mainly responsible for this dimerization.

FIM-FGFR1 Protein Induces Limited Ligand-independent Cell Survival of Ba/F3 Cells—The biological responses of the FIM-FGFR1 fusion protein were studied in the murine hematopoietic cell line Ba/F3. In this cell model, which does not express endogenous FGFR1 (data not shown), a transfected FGFR1 in the presence of its ligand sustains cell survival and growth after IL-3 withdrawal (29). In the analyses described below, cells expressing FGFR1 were cultured in the presence of FGF1 and heparin (see "Experimental Procedures"). Expression of the FGFR1 or of FIM-FGFR1 in various stable transfectant clones was analyzed by Western blot analysis. Representative results are shown in Fig. 6. FGFR1 was strongly expressed in FGFR1 clones, whereas a low level of expression of FIM-FGFR1 was found in mutant clones.

To characterize the cell growth characteristics associated with FIM-FGFR1 expression, we studied the DNA content of expressing cells by fluorescence-activated cell sorter analysis. In the presence of IL-3, there was no significant difference in the percentage of viable cells transfected with either empty vector or FIM-FGFR1 (Table I) nor in the cell cycle profiles (Fig. 7*A*, *panels b* and *d*). In contrast, in the absence of IL-3, the number of viable cells and cell cycle profiles of the respective clones were significantly different. As shown in Table I, by 72 h of culture the percentage of viable cells transfected with vector alone was 7%, whereas that of FIM-FGFR1-expressing cells ranged from 20 to 34% and that of FGFR1 cells was 34%. Similar results were obtained when cell growth was monitored by cell counting (data not shown). These results showed that FIM-FGFR1 is able to promote cell survival in the absence of IL-3.

The number of hypodiploid cells assessed by fluorescence-activated cell sorter analysis (sub-G_1 phase) is known to be associated with cell apoptosis (30). Analysis of cell cycle profiles showed that the percentage of empty vector transfected cells with a sub-G1 DNA content drastically increased from 24 h in culture after IL-3 withdrawal (Fig. 7*B*, *panels a* and *b*). In contrast, no significant difference was observed for FIM-FGFR1 cells in sub-G1 in the presence or absence of IL-3 (Fig. 7, *A* and *B*, *panels c* and *d*) or for FGFR1-expressing cells (Fig. 7, *A* and *B*, *panels e* and *f*), confirming the positive effect FIM-FGFR1 on cell survival. In addition, compared with FGFR1, no IL-3 independent proliferation of FIM-FGFR1 transfectant cells was seen (data not shown). The fusion protein could therefore sustain cell survival by preventing apoptosis of Ba/F3 cells, whereas ligand-activated FGFR1 induces both cell survival and sustained proliferation.

DISCUSSION

FIM-FGFR1 is the chimeric product of the t(8;13) translocation associated with a stem cell myeloproliferative disorder. This fusion protein contains the FIM zinc finger motifs and the catalytic domain of the tyrosine kinase receptor FGFR1.

FIM-FGFR1 Is Cytoplasmic, and FIM Is Nuclear—One important issue in characterizing the functional properties of a translocation product is to determine its subcellular localization. Many chromosomal translocations that generate constitutively activated kinases lead to a delocalization of the fusion protein compared with its normal counterpart (33, 34). We have shown here that the same occurs with FIM-FGFR1; whereas the wild type FIM protein is nuclear and nucleolar, the FIM-FGFR1 protein localizes to the cytoplasm. Thus, FIM-FGFR1 may affect cell growth through two combined dysregulations, *i.e.* continuous kinase stimulus and recruitment of signaling molecules not normally involved in FGFR1 signaling. Lack of recruitment of normal FGFR1 substrates, such as SNTs, may also be important to FIM-FGFR1 activity, in switching off the RAS pathway (35, 36).

FIM Colocalizes with UBF in the Nucleolus at Interphase—The precise subcellular localization of FIM was also examined to gather some insights about its unknown function. Our immunofluorescence data on either transfected or untransfected cells show that FIM is localized in the nucleus and the nucle-

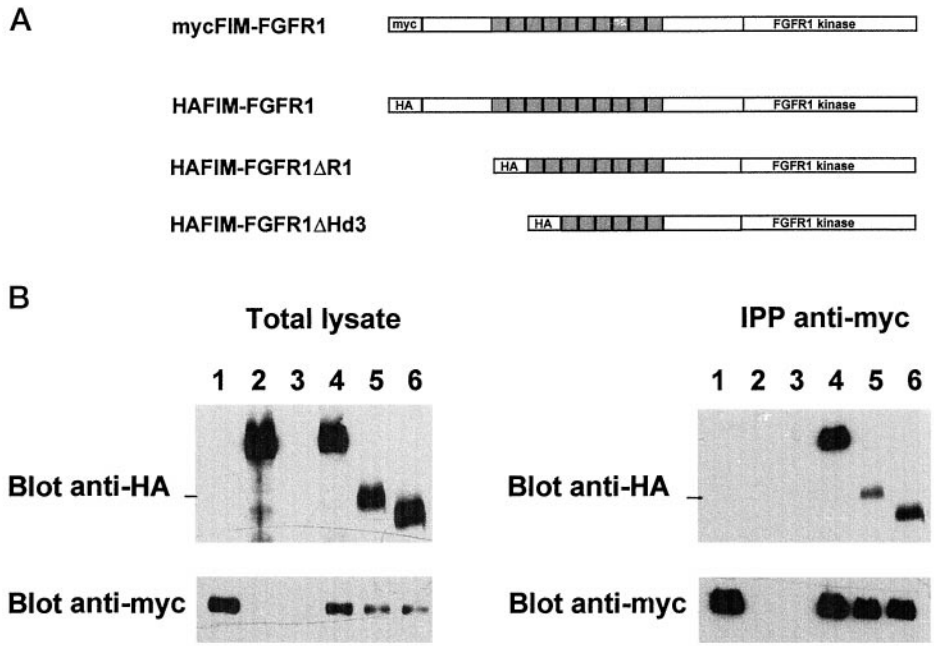

FIG. 5. **Dimerization of FIM-FGFR1 in Cos-1 cells.** Two differently tagged FIM-FGFR1 constructs (Myc and HA) were made, and dimerization between a Myc-tagged and an HA-tagged FIM-FGFR1 protein was studied following overexpression in Cos-1 cells and immunoprecipitation with anti-Myc antibody. *A* shows schematically the different constructs that were made in the pcDNA3 expression vector: a full-length mycFIM-FGFR1, a full-length HAFIM-FGFR1, and two N-terminal deletions, HAFIM-FGFR1ΔR1 and HAFIM-FGFR1ΔHd3, maintaining eight and six zinc fingers of the FIM region, respectively. These constructs were transfected in Cos-1 cells in different combinations. 24 h after transfection, total cell lysates (*B*, *left*) or anti-Myc immunoprecipitates (*B*, *right*) were analyzed by SDS-gel electrophoresis followed by immunoblotting with either anti-HA or anti-Myc antibody. *B* shows the results of Western blot from Cos-1 cells transfected with 10 μg of mycFIM-FGFR1 (*lane 1*), 10 μg of HAFIM-FGFR1 (*lane 2*), 10 μg of empty vector pCDNA3 (*lane 3*), 5 μg of mycFIM-FGFR1 + 5 μg of HAFIM-FGFR1 (*lane 4*), 5 μg of mycFIM-FGFR1 + 5 μg of HAFIM-FGFR1ΔR1 (*lane 5*) and 5 μg of mycFIM-FGFR1 + 5 μg of HAFIM-FGFR1ΔHd3 (*lane 6*).

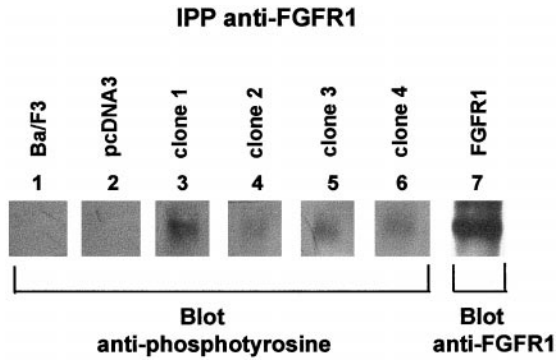

FIG. 6. **Expression pattern of stable transfected Ba/F3 clones.** Cell lysates from 2×10^6 Ba/F3 cells were immunoprecipitated with anti-C-FGFR1 antibody and analyzed by Western blotting with either anti-phosphotyrosine or anti-C-FGFR1 antibodies as indicated. Lysates were prepared from different Ba/F3 clones: untransfected Ba/F3 (*lane 1*) or Ba/F3 cells from clones stably transfected with pcDNA3 vector (*lane 2*), FIM-FGFR1 (four different clones, *lanes 3–6*), or wild type FGFR1 (*lane 7*).

olus, suggesting that it may play some role in transcription or gene regulation. Moreover, we observed a colocalization of nucleolar FIM with the upstream binding factor, one of the transacting factors required for efficient transcription of rDNA by RNA polymerase I (31). This colocalization was seen during interphase but not in mitotic cells when transcription of rRNA genes is shut off (24), indicating that FIM proteins could have some regulatory role on either rRNA synthesis or maturation.

FIM and FIM-FGFR1 Dimerize in Vitro and in Vivo—Whereas the C terminus of FIM is responsible for its nuclear and nucleolar subcellular localization, we demonstrate by two different approaches that the N terminus is important for dimerization. We showed that FIM sequences containing four zinc finger motifs can mediate efficient dimerization. Therefore, the FIM N-terminal region present in the chimeric protein is able to induce its dimerization leading to the constitutive activation of the FGFR1 kinase. It is likely that such a mechanism of activation is also involved for the two other chimeric proteins found in the 8p11 myeloproliferative disorder. Indeed, in this disorder, the nonkinase partners of FGFR1, FOP (4), and CEP110[1] contain in their respective N-terminal region leucine-rich repeats and leucine zippers motifs known to be capable of mediating dimerization. Therefore, the fusion partners of FGFR1 in these translocations appear to be required to juxtapose a dimerization domain N-terminal of the FGFR1 kinase, inducing in this manner its constitutive activity. This phenomenon has been shown to be involved in a number of neoplasia-associated tyrosine kinase (37, 38). It has also been shown that the ligand-independent activation of FGFR1 leads to a constitutively active form responsible for oncogenic transformation (39).

FIM and FIM-FGFR1 are able, in theory, to dimerize *in vivo*. However, because we have shown that they are localized in different subcellular compartments, it is unlikely that FIM-

TABLE I
Cell survival

Shown are the percentages of viable cells calculated from flow cytometric measurements of the DNA content. Cells were stably transfected by pcDNA3, FIM-FGFR1 (four clones, see Fig. 6), or FGFR1 and cultured with (+) or without (−) IL-3 for the time period indicated. Three independent experiments were done, and similar results were obtained.

Clones	6 h		24 h		48 h		72 h	
	+	−	+	−	+	−	+	−
pcDNA3	86	85	76	54	64	12	57	7
FIM-FGFR1 (1)	75	71	77	79	78	58	67	25
FIM-FGFR1 (2)	88	70	71	67	64	40	59	20
FIM-FGFR1 (3)	74	73	74	69	66	53	53	27
FIM-FGFR1 (4)	68	69	72	74	83	54	66	34
FGFR1	67	72	68	71	46	44	33	34

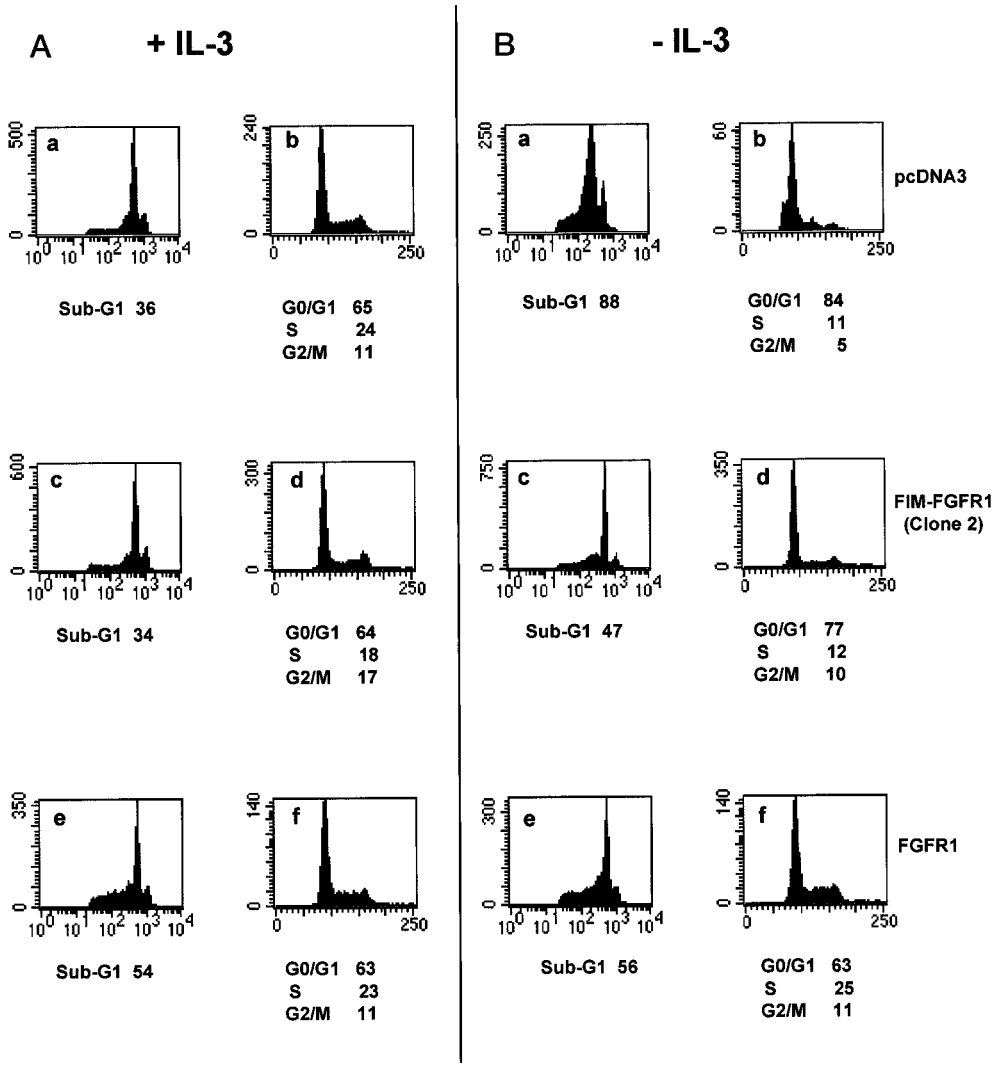

FIG. 7. **Flow cytometric analyses of Ba/F3 transfected cells.** The flow cytometry profiles show DNA fluorescence of propidium iodide-stained Ba/F3 cell nuclei cultured 48 h in the presence (*A*) or absence (*B*) of IL-3. Cells were stably transfected with pcDNA3 vector (*top panels*), FIM-FGFR1 (*middle panels*), or FGFR1 (*bottom panels*). The cell cycle phase distribution was calculated from flow cytometric measurements of the DNA content. This is a representative experiment of three, all of which gave similar results.

FGFR1 oncogenic property is mediated through such an heterodimerization.

FIM-FGFR1 Expression Induces Cell Survival—Based on the knowledge that FGFR1 activation leads to cell survival and growth in the pro-B Ba/F3 cell line (29), we explored the cell growth properties of Ba/F3 cells expressing FIM-FGFR1. Our results show that FIM-FGFR1 supports cell survival following IL-3 withdrawal. However, FIM-FGFR1-expressing Ba/F3 cells did not proliferate in the absence of IL-3, suggesting that the fusion protein is only able to activate a partial FGFR1 response. Similar results have been recently reported in skeletal muscle cells in which the FGFR1 kinase domain regulates myogenesis differentiation but does not stimulate cell proliferation (40).

Factors such as IL-3 not only stimulate cell growth but are also necessary for survival of hematopoietic cells (41). IL-3-dependent survival is known to rely on the activity of multiple signaling pathways leading to activation of phosphoinositide 3-kinase and the protein kinase AKT (42), an important component of a cell survival pathway (43). Effect on cell survival rather than cell proliferation has been well documented for the product of *E2A-HLF*, the fusion gene formed by the t(17;19) chromosomal translocation involved in the leukemic transformation of early B-cell precursors (44). We cannot rule out that a stronger Ba/F3 response could be obtained with a higher expression of FIM-FGFR1. However, we were able to isolate only low expressing FIM-FGFR1 clones; this may reflect a toxic effect of the fusion protein. Alternatively, the limited effect of FIM-FGFR1 may signify that Ba/F3 cells, despite being hematopoietic cells, are not a truly relevant cell culture system for assaying its potential. The FIM-FGFR1 oncogenic effect could be restricted to permissive cells, which may be the hematopoietic stem cells only, as demonstrated for other fusion proteins (45).

In conclusion, FIM-FGFR1 may participate in the malignant process through two combined dysregulations, *i.e.* continuous kinase stimulus and abnormal recruitment of signaling molecules because of both its cytoplasmic localization and modified structure, and this may result in uncoupling apoptosis from other cell regulatory signals.

Acknowledgments—We are grateful to D. Maraninchi and C. Mawas for help and encouragement.

REFERENCES

1. MacDonald, D., Aguiar, R. C., Mason, P. J., Goldman, J. M., and Cross, N. C. (1995) *Leukemia* **9,** 1628–1630
2. Chaffanet, M., Popovici, C., Leroux, D., Jacrot, M., Adélaïde, J., Dastugue, N., Grégoire, M.-J., Lafage Pochitaloff, M., Birnbaum, D., and Pébusque, M.-J. (1998) *Oncogene* **16,** 945–949

3. Johnson, D. E., and Williams, L. T. (1993) *Adv. Cancer Res.* **60,** 1–41
4. Popovici, C., Zhang, B., Grégoire, M.-J., Jonveaux, P., Lafage-Pochitaloff, M., Birnbaum, D., and Pébusque, M.-J. (1999) *Blood* **93,** 1381–1389
5. Popovici, C., Adélaïde, J., Ollendorff, V., Chaffanet, M., Guasch, G., Jacrot, M., Leroux, D., Birnbaum, D., and Pébusque, M.-J. (1998) *Proc. Natl. Acad. Sci. U. S. A.* **95,** 5712–5717
6. Reiter, A., Sohal, J., Kulkarni, S., Chase, A., MacDonald, D. H., Aguiar, R. C., Goncalves, C., Hernandez, J. M., Jennings, B. A., Goldman, J. M., and Cross, N. C. (1998) *Blood* **92,** 1735–1742
7. Xiao, S., Nalabolu, S. R., Aster, J. C., Ma, J., Abruzzo, L., Jaffe, E. S., Stone, R., Weissman, S. M., Hudson, T. J., and Fletcher, J. A. (1998) *Nat. Genet.* **18,** 84–87
8. Smedley, D., Hamoudi, R., Clark, J., Warren, W., Abdul-Rauf, M., Somers, G., Venter, D., Fagan, K., Cooper, C., and Shipley, J. (1998) *Hum. Mol. Genet.* **7,** 637–642
9. van der Maarel, S., Scholten, I., Huber, I., Philippe, C., Suijkerbuijk, R., Gilgenkrantz, S., Kere, J., Cremers, F., and Ropers, H. (1996) *Hum. Mol. Genet.* **5,** 887–897
10. Still, I. H., and Cowell, J. K. (1998) *Blood* **92,** 1456–1458
11. Sawyers, C. L., Denny, C. T. (1994) *Cell* **77,** 171–173
12. Popovici, C., Ollendorff, V., Coulier, F., Pébusque, M.-J., and Birnbaum, D. (1998) *Hématologie* **4,** 361–369
13. Schlessinger, J. (1988) *Trends Biochem. Sci.* **13,** 443–447
14. Mackay, J., and Crossley, M. (1998) *Trends Biochem. Sci.* **23,** 1–4
15. Palacios, R., and Steinmetz, M. (1985) *Cell* **41,** 727–734
16. Mathey-Prevot, B., Nabel, G., Palacios, R., and Baltimore, D. (1986) *Mol. Cell. Biol.* **6,** 4133–4135
17. Evan, G. I., Lewis, G. K., Ramsay, G., and Bishop, J. M. (1985) *Mol. Cell. Biol.* **5,** 3610–3616
18. Munro, S., and Pelham, H. R. (1986) *Cell* **46,** 291–300
19. Ollendorff, V., and Donoghue, D. J. (1997) *J. Biol. Chem.* **272,** 32011–32018
20. Bellot, F., Crumley, G., Kaplow, J. M., Schlessinger, J., Jaye, M., Dionne, C. A. (1991) *EMBO J.* **10,** 2849–2854
21. Borg, J.-P., Ooi, J., Levy, E., and Margolis, B. (1996) *Mol. Cell. Biol.* **16,** 6229–6241
22. Dionne, C., Crumley, G., Bellot, F., Kaplow, J., Searfoss, G., Ruta, M., Burgess, W., Jaye, M., and Schlessinger, J. (1990) *EMBO J.* **9,** 2685–2692
23. Roussel, P., André, C., Masson, C., Géraud, G., and Hernandez-Verdun, D. (1993) *J. Cell Sci.* **104,** 327–337
24. Roussel, P., André, C., Comai, L., and Hernandez-Verdun D. (1996) *J. Cell Biol.* **133,** 235–246
25. Gaugain, B., Barbet, J., Oberlin, R., Roques, B. P., and Le Pecq, J. B. (1978) *Biochemistry* **17,** 5071–5078
26. Gaugain, B., Barbet, J., Capelle, N., Roques, B. P., and Le Pecq, J. B. (1978) *Biochemistry* **17,** 5078–5088
27. Vojtek, A. B., Hollenberg, S. M., and Cooper, J. A. (1993) *Cell* **74,** 205–214
28. Vojtek, A. B., and Hollenberg, S. M. (1995) *Methods Enzymol.* **255,** 331–342
29. Wang, J. K., Gao, G., and Goldfarb, M. (1994) *Mol. Cell. Biol.* **14,** 181–188
30. Nicoletti, I., Migliorati, G., Pagliacci, M. C., Grignani, F., and Riccardi, C. (1991) *J. Immunol Methods* **139,** 271–279
31. Hannan, K. M., Ross, R. D., and Rothblum, L. I. (1998) *Front. Biosci.* **3,** 376–398
32. Zatsepina, O. V., Voit, R., Grummt, I., Spring, H., Semenov, M. V., and Trendelenburg, M. F. (1993) *Chromosoma* **102,** 599–611
33. Rodrigues, G. A., and Park, M. (1994) *Curr. Opin. Genet. Dev.* **4,** 15–24
34. Look A. T. (1998) *The Genetic Basics of Human Cancer* (Vogelstein, B., and Kinzler, K. W., eds) pp. 109–141, McGraw-Hill Inc., New York
35. Wang, J. K., Xu, H., Li, H. C., and Goldfarb M. (1996) *Oncogene* **13,** 721–729
36. Xu, H., Lee, K. M., and Goldfarb M. (1998) *J. Biol. Chem.* **273,**17987–17990
37. Bongarzone, I., Monzini, N., Borrello, M. G., Carcano, C., Ferraresi, G., Arighi, E., Mondellini, P., Della Porta, G., and Pierotti, M. A. (1993) *Mol. Cell. Biol.* **13,** 358–366
38. Golub, T. R., Goga, A., Barker, G. F., Afar, D. E., McLaughlin, J., Bohlander, S. K., Rowley, J. D., Witte, O. N., and Gilliland, D. G. (1996) *Mol. Cell. Biol.* **16,** 4107–4116
39. Kouhara, H., Kurebayashi, S., Hashimoto, K., Kasayama, S., Koga, M., Kishimoto, T., and Sato, B. (1995) *Oncogene* **10,** 2315–2322
40. Kudla, A. J., Jones, N. C., Rosenthal, R. S., Arthur, K., Clase, K. L., and Olwin, B. B. (1998) *J. Cell Biol.* **13,** 241–250
41. Thompson, C. B. (1995) *Science* **267,** 1456–1462
42. Franke, T. F., Kaplan, D. R., and Cantley, L. C. (1997) *Cell* **88,** 435–437
43. Songyang, Z., Baltimore, D., Cantley, L. C., Kaplan, D. R., and Franke, T. F. (1997) *Proc. Natl. Acad. Sci. U. S. A.* **94,** 11345–11350
44. Inaba, T., Inukai, T., Yoshihara, T., Seyschab, H., Ashmun, R. A., Canman, C. E., Laken, S. J., Kastan, M. B., and Look, A. T. (1996) *Nature* **382,** 541–544
45. Barr, F. G. (1998) *Nat. Genet.* **19,** 121–124

Characterization of FIM-FGFR1, the Fusion Product of the Myeloproliferative Disorder-associated t(8;13) Translocation

Vincent Ollendorff, Géraldine Guasch, Daniel Isnardon, Rémy Galindo, Daniel Birnbaum and Marie-Josèphe Pébusque

J. Biol. Chem. 1999, 274:26922-26930.
doi: 10.1074/jbc.274.38.26922